ACTA ASTRONOMICA
Vol. **47** (1997) pp. 263–280

Spectral Components in the Optical Emission of the Seyfert Galaxy NGC 5548 and the Comparison of Intrinsic Nuclear Spectra with Accreting Corona Model

by

J. Kuraszkiewicz, Z. Loska, and B. Czerny

Copernicus Astronomical Center, Bartycka 18, 00-716 Warsaw, Poland
e-mail:(jcuk,zbylo,bcz)@camk.edu.pl

Received May 7, 1997

ABSTRACT

We study the extensively monitored Seyfert galaxy NGC 5548 and compare its nuclear emission with models of accretion disk with accreting corona. To obtain the intrinsic nuclear spectra from the observed spectra we had to estimate and subtract the contribution from circumnuclear components such as stars, the Balmer continuum and blended FeII lines, and the FC2 extended, featureless continuum. The true nuclear spectra were compared with a two parameter model of the accreting disk with an accreting corona, described by the mass of the central black hole and viscosity. The model that best fitted the data was for $M_{BH} = 1.4 \times 10^8 \mathrm{M}_\odot$ and the viscosity parameter $\alpha = 0.033$. Such a low viscosity parameter was necessary to produce the sufficient amount of X-rays. The vertical outflow of mass from corona in the form of wind had to be neglected in our model in order to fit into high and low states that NGC 5548 underwent. The model also predicts the behavior of the overall opt/UV/X continuum of NGC 5548 during the whole five year campaign.

Key words: *Galaxies: active – Galaxies: Seyfert – Galaxies: individual: NGC 5548 – Accretion, accretion disks*

1. Introduction

The Seyfert 1 galaxy NGC 5548 ($z = 0.0174$) is one of a few active galaxies extensively and systematically monitored over the last ten years as its nucleus is strongly variable, bright, and the galaxy is relatively nearby. The amount of data collected for NGC 5548 actually exceeds all the other monitored AGN: NGC 3783 (Reichert *et al.* 1994, Stripe 1994), Mrk 335 (Zheng *et al.* 1995) or the BL Lac object PKS 2155-304 (Edelson *et al.* 1995).

The galaxy has been frequently observed since late seventies in the optical band, in the UV with IUE, and by a number of X-ray satellites. In 1988 a systematic campaign has been started by AGN Watch team. Optical spectra were taken by ground based telescopes every ~ 4 days since December 1988 (Peterson *et al.* 1991,

1992, 1994). UV variability was followed with IUE during first eight months of the campaign (December 1988 – August 1989) with the same frequency sampling (Clavel *et al.* 1991). The X-rays and UV were measured simultaneously by IUE and Ginga satellite 11 times (Clavel *et al.* 1992). In 1993 the galaxy was monitored by HST and IUE in the UV band (Korista *et al.* 1995). Soft X-ray variability was monitored by EUVE satellite (Marshall, Fruscione and Carone 1995) as well as ROSAT (*e.g.*, Done *et al.* 1995).

The collected data have been used for a number of studies of relative delays in various energy bands (optical *vs.* UV, X-rays *vs.* opt and UV etc.) as well as between the continuum and the broad emission lines. These data offer also an unprecedented possibility to study the variability of the nuclear continuum thus offering a chance to distinguish between the variety of models able to represent the average overall continuum in a typical Seyfert galaxy (*e.g.*, Loska and Czerny 1997).

However, the continuum models can be tested against the data only if we are able to determine the observed continuum emission of the nucleus. It means that the observed continuum has to be decomposed into true nuclear emission and contributions from circumnuclear components.

This additional continuum emission clearly consists of the (variable) contribution from the Balmer continuum and blended FeII lines emitted by the Broad Line Region (BLR) (*e.g.*, Wills, Netzer and Wills 1985) and from the stars located at a distance of a few hundreds of parsecs from the nucleus (*e.g.*, Yee and Oke 1978). It was suggested, however, that also the third component is present, much bluer than the starlight and rather similar to the true nuclear continuum but coming from extended region (*e.g.*, Antonucci 1993, Tran 1995). Since both this component and the true nuclear emission are featureless, the two components are called FC2 and FC1, correspondingly.

In this paper we attempt to make a decomposition of the optical continuum of NGC 5548 derived during the monitoring campaign into nuclear emission and the remaining three components listed above. Whenever possible, we use two methods at every stage, to ensure that the decomposition does not depend strongly on the adopted method. Such a decomposition opens the way to subsequent modeling of the variability of the nuclear continuum.

The outline of the paper is the following. In Section 2 we discuss the contribution of starlight to the data and we derive its relative normalization from aperture effects as well as from the depth of absorption features. In Section 3 we derive the contamination by the FC2 component from the relation between H_β line and the true nuclear continuum at 5100 Å. Finally, the true nuclear emission in the optical/UV band is presented in Section 4. We compare it with the predictions of the model of an accretion disk with accreting corona. The discussion is given in Section 5.

2. Contamination by Starlight

The optical data collected during the monitoring campaign are described in a series of papers by Peterson *et al.* (1991, 1992, 1994). The data are available to the astronomical community due to the courtesy of the AGN Watch team. The spectra are calibrated using standard software for each telescope. However, as different telescopes and apertures were used, secondary calibration is needed in order to reduce all the spectra to the set A with aperture $5\farcs0 \times 7\farcs6$. We performed this reduction following the description given by Peterson *et al.* (1994), *i.e.*, we used values of ϕ (a point-source correction factor) and G (starlight correction factor at 5100 Å) appropriate for a given set of data, calibrated to the mean [OIII] (λ5007) flux. We transformed the spectra to the rest frame and we also corrected the spectra for the effect of interstellar extinction. The reddening is not significant – we adopted the value of $E(B-V)$ equal to 0.05, as inferred from the neutral hydrogen column (Burstein and Heiles 1984) in the direction of this galaxy, although even smaller value 0.035 was recently used by some authors (*e.g.*, Reynolds 1997). We deredden the spectra using the standard Seaton extinction curve (Seaton 1979). It results in the increase of the flux at 5100 Å by a factor of 1.174 and at 1350 Å by a factor of 1.499. We adopted these values in further computations. Spectra prepared in such a way were used to determine the amount of starlight in the standard set A aperture.

2.1. Stellar Absorption Lines

The fraction of light due to stars can be estimated from the ratio of the observed equivalent widths of stellar absorption lines to their average value in the spectrum of a template galaxy, which we take to be the spectrum of the nuclear bulge of M31, after Coleman *et al.* (1980), Table 2. We have used this galaxy as a template since it was shown by Wamsteker *et al.* (1990) that the starlight spectrum of NGC 5548 is similar to the starlight spectrum of M31.

For the purpose of starlight estimation, the spectrum n58733h from day 8733 (JD minus 2,440,000) from set H of Peterson *et al.* (1994) was used. As spectra from this set have the broadest wavelength coverage (together they cover from 3000 Å to 10,000 Å), more absorption features could be identified. It was also important that the spectrum came from the epoch at which the galaxy reached its minimum so the contribution of starlight to the total flux was more pronounced. At day 8733 the nucleus was rather dim with the total flux at 5100 Å of 6.48×10^{-15} ergs/s/cm^2/Å. The minimum of F_λ during the entire 1988–1994 campaign was equal to 5.70×10^{-15} ergs/s/cm^2/Å (day 8816).

The n58733h spectrum was normalized by dividing the flux by the local value of continuum (obtained by fitting a spline to the spectrum). A similar procedure was applied to the template starlight galaxy. This method removed broad band trends from the continuum of these spectra and showed the absorption features more clearly. In Fig. 1 the normalized spectrum n58733h is presented together with the normalized template galaxy M31.

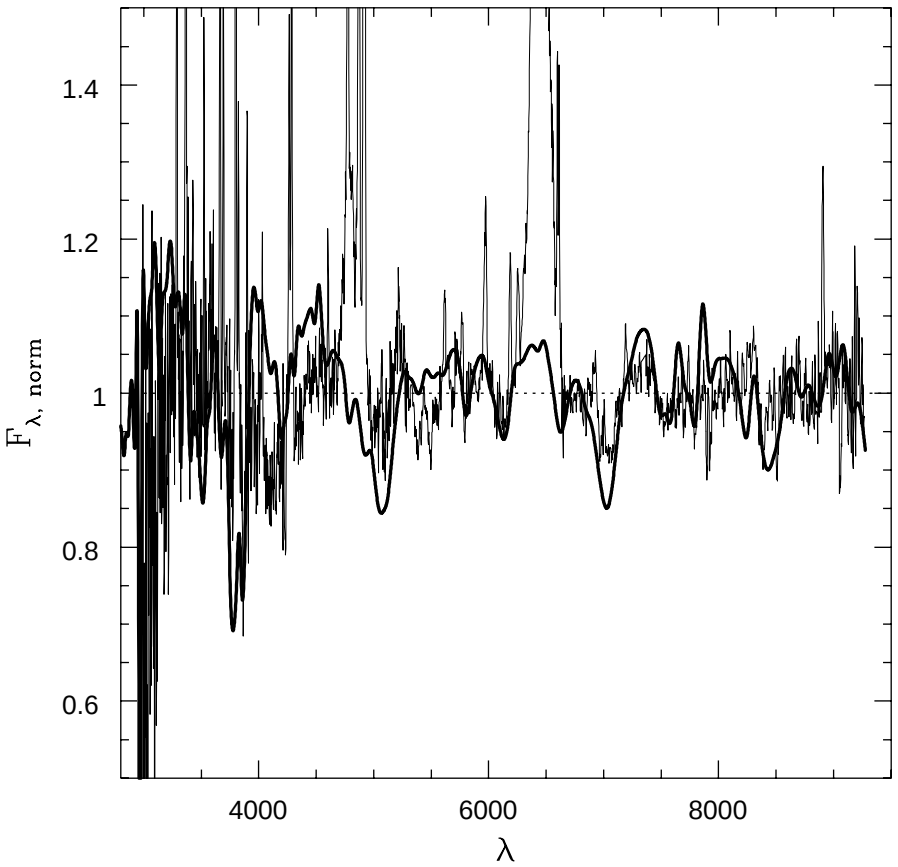

Fig. 1. The spectrum of NGC 5548 (n58733, thin line) and the template starlight galaxy M31 (thick line), both normalized as described in Section 2.1.

The spectroscopic indicators of stellar population are prominent absorption lines such as: the CaII H (λ3968) and CaII K (λ3934) line and NaI D (λ5890,5896) line which are often contaminated by interstellar absorption in the host galaxy. Other absorption features such as the CaII G (λ4304) and the MgI b triplet (λ5167,5173,5184) are usually contaminated by the nearby emission lines (the CaII by H_γ and the MgI by NI) so these lines were not used for starlight estimation. The lines that were used are: FeI+CaI (λ6129,6072) and FeI (λ7406,7458,7511). In Table 1 we show the percentage of starlight estimated from different absorption features and defined as the EW of an absorption feature in the spectrum to the EW of the same feature in the template starlight galaxy M31. Next we calculate the amount of starlight at 5100 Å in absolute units taking into account the spectral shape of both the starlight and the combined starlight plus nuclear emission. The value estimated from the FeI+CaI ($\sim$ 6100 Å) feature is 3.4×10^{-15} ergs/s/cm^2/Å and estimated from the FeI ($\sim$ 7500 Å) feature is 3.3×10^{-15} ergs/s/cm^2/Å. The estimate of starlight contribution based on spectral features does not include the

T a b l e 1

starlight feature	% of starlight	remarks
FeI(4923, 5018,5169), MgI+MgH	5.8%	MgI contaminated by NI
NaI(5890,5896)		emission
FeI+CaI(6072,6129)	52.8%	
CaH(6934),FeI(7008,7109,7157)	12.9%	CaH contamination by ISM
FeI(7459,7511)	64%	
CaII (8498,8542)	11 %	contamination by ISM

possible contribution from featureless FC2 component. It is therefore particularly interesting to compare it with the determination of starlight by aperture methods which may include most of its contribution if this component is extended.

2.2. Comparison with Aperture Estimates

Another estimation of starlight can be made by comparing spectra obtained through different apertures. By subtracting a small aperture spectrum from a large aperture spectrum we can obtain off-nuclear emission from the circumnuclear ring which should be entirely due to starlight. We found a few pairs of observations made with distinctively different apertures and separated in time not more than four days, so the variations of the flux were relatively unimportant. It was also crucial for the different aperture spectra to have large wavelength coverage as to obtain the shape of starlight over a broad wavelength range. Spectra which best fitted the above criteria were those from set F (aperture $3\overset{''}{.}2 \times 6\overset{''}{.}4$) and H (aperture $4\overset{''}{.}0 \times 10\overset{''}{.}0$) which together covered 4500 Å to 7000 Å. An example of an off-nuclear spectrum obtained from the subtraction of spectra from these sets (n58765h minus n58765f) is shown in Fig. 2, together with the template galaxy M31 used in the Section 2.1. The "starlight" obtained in such a way is much steeper than the template starlight and shows a prominent H_α line. The cause of such steepening is the fact that in the Peterson *et al.* (1994) data the spectra at different apertures were obtained with different telescopes and most probably the original reduction of the data from the small aperture (the 1.6 m Mount Hopkins observations) was much too simplistic (D. Dobrzycka, private communication).

The available data did not allow for the determination of starlight based on different aperture spectra. It also showed that broad band optical spectra are not calibrated well enough to use for comparison with the models. In further Sections we constrain ourselves to spectra from set A or fluxes at 5100 Å for the purpose of modeling. Because data from these sets do not cover the wavelength range of the Balmer continuum and the FeII emission lines we do not need to worry about this contribution in the spectra in further analysis.

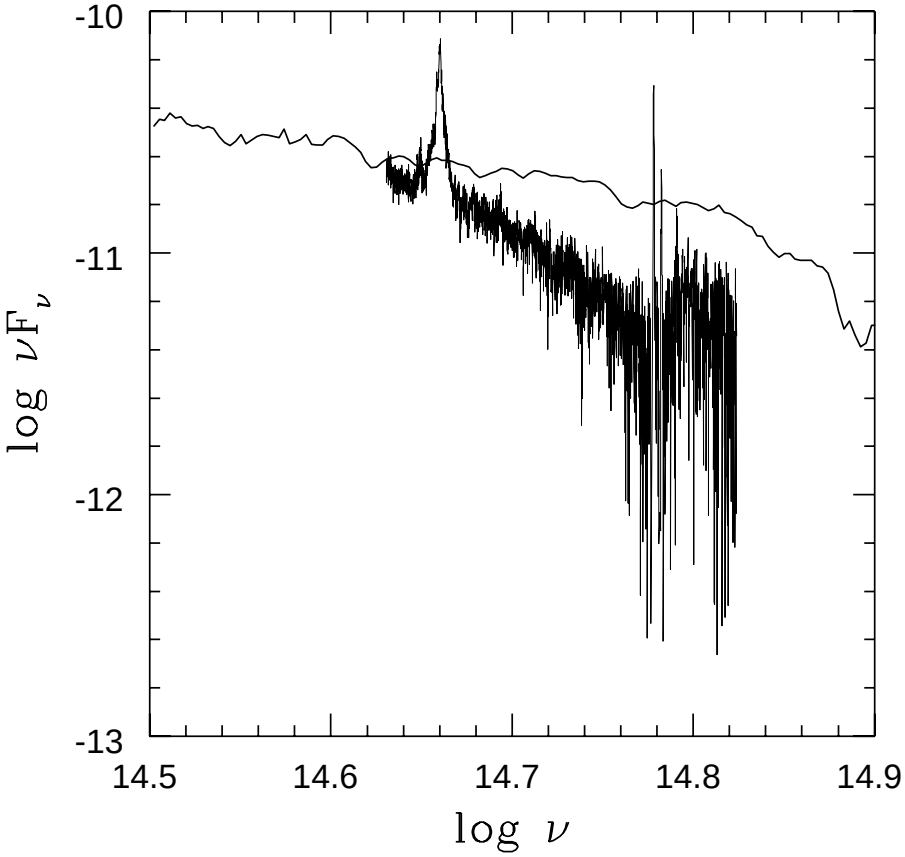

Fig. 2. The off-nuclear spectrum of NGC 5548 calculated by subtraction of the observation n58765f (aperture $3\farcs2 \times 6\farcs4$) from n58765h (aperture $4\farcs0 \times 10\farcs0$). It differs considerably from the overall shape of the starlight template (given with arbitrary normalization).

Much better attempt was made by Romanishin *et al.* (1995), who using a single telescope made direct imaging of NGC 5548. The authors obtained the value of 3.4×10^{-15} ergs/s/cm^2/Å for starlight at F_λ(5100 Å) (for aperture $5'' \times 7\farcs6$) which is identical with the value of $3.37 \pm 0.54 \times 10^{-15}$ ergs/s/cm^2/Å found from comparison of IUE and 5100 Å fluxes by Peterson *et al.* (1991). This method gave the same value of starlight as the method based on stellar absorption features (see previous Section).

The method of estimating starlight based on absorption features is more reliable in the case of using high quality nuclear and off-nuclear spectra of the same galaxy obtained with the same telescope (*e.g.*, Serote-Ross *et al.* 1996 for NGC 3516). For NGC 5548 off-nuclear data are not available and simple use of templates from another galaxy may lead to highly uncertain results.

However, since the outcome of our absorption feature method coincides well with the aperture based results of Romanishin *et al.* (1995) we can safely use the value 3.4×10^{-15} ergs/s/cm^2/Å of starlight in further analysis.

3. Contribution from Extended Featureless Continuum FC2

The monitoring of NGC 5548 showed that the continuum of this galaxy as well as the H_β flux varies strongly with time. We use this phenomenon to estimate the amount of the extended featureless continuum FC2 within the standard set A spectra.

The broad H_β line is found to vary in response to continuum variations with a lag of about 20 days, which varies from year to year. Fig. 3 presents the dependence of H_β flux (corrected for Galactic reddening) from optical flux at 5100 Å (corrected for Galactic reddening and starlight contamination). The H_β fluxes were shifted in time by 18 days – the mean delay of the campaign.

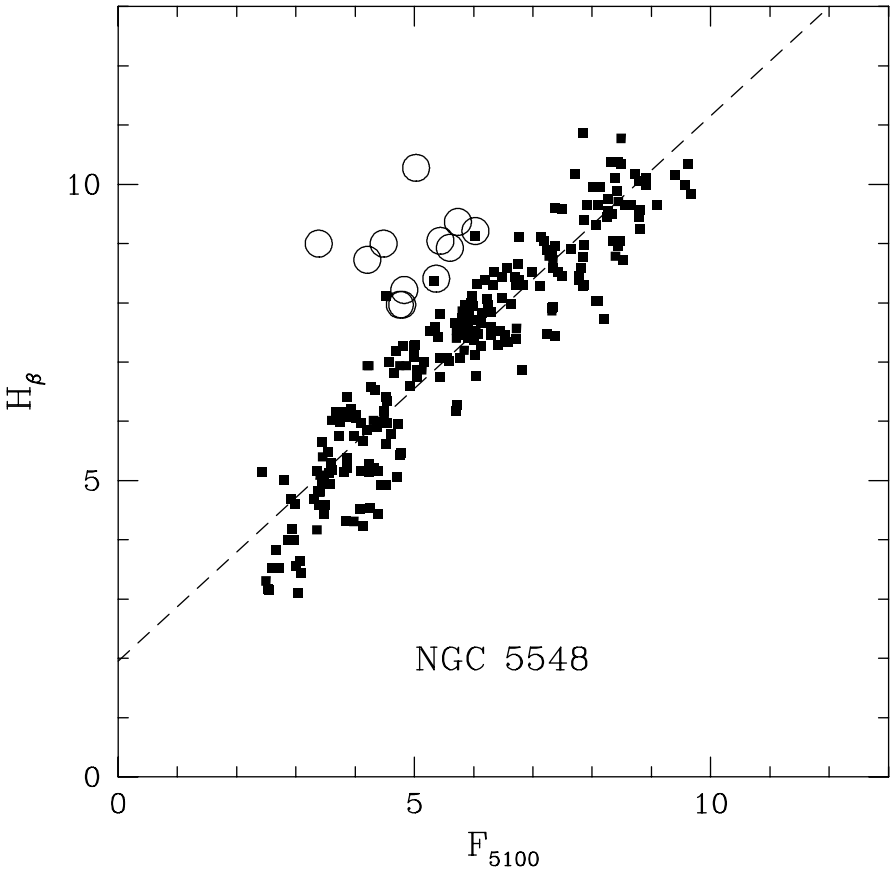

Fig. 3. The dependence of the H_β flux measured in units of 10^{-13} erg/s/cm^2 on the continuum flux at 5100 Å measured in units of 10^{-15} erg/s/cm^2/Å (after starlight subtraction). Both fluxes were dereddened. The data cover the first four years of the campaign (Peterson *et al.* 1994). Points marked by large open circles come from the four week sequence in July/August 1989 and were not included in the linear fit to the trend (dashed line).

Apart from the short sequence marked with large circles (dates from 7728 to 7766), the H_β line responds almost linearly to the underlying continuum.

The H_β line consists of components originating in the broad line region and in the narrow line region. The component that is sensitive to short-time nuclear continuum changes is the component that lies nearest to the central engine, *i.e.*, the H_β^{BLR}. The remaining H_β components originate from the Narrow Line Region (NLR) that lies further away (the distance to the NLR is of order of a hundred light years) and is not subject to such changes.

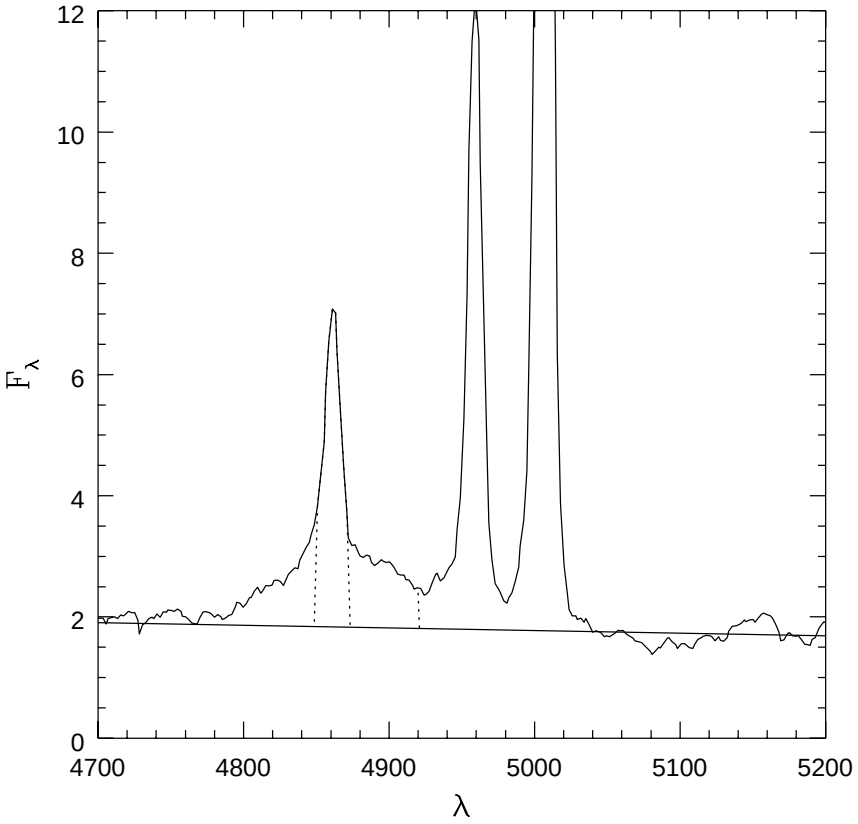

Fig. 4. Decomposition of the H_β profile into broad and narrow components in the data 8733, taken when the source was faint. A power law continuum was adopted, normalized outside the spectral band dominated by strong emission lines.

We estimated the value of H_β^{NLR} by decomposing the line profile into two components: a broad line and a narrow line (see Fig. 4). We used for that purpose the spectrum n58733a (day 8733) as the broad components during that epoch were weak and the relative contribution from the narrow components was high, which allowed for relatively accurate decomposition. The value of 1.5×10^{-13} erg/s/cm^2 for the narrow component was obtained.

We compared this value with the value expected on statistical grounds. The amount of H_β originating from the narrow line region can be estimated based on paper by Osterbrock (1989), who showed that the logarithm of the ratio of H_β to [OIII] flux in the NLR for Seyfert galaxies is in the – 0.3 to 1 range. The value

of $0.35 - 11.1 \times 10^{-13}$ ergs/s/cm^2 is obtained assuming that the [OIII] flux for NGC 5548, as inferred from large-aperture observations (Peterson *et al.* 1991), is 5.58×10^{-13} erg/s/cm^2. Since the observed angular size corresponds to 340 pc per arcsec ($z = 0.0174$, $d = 70$ Mpc for $H_0 = 75$ km/s/Mpc) the size of the region observed in the standard A aperture is 1.7 kpc $\times$ 2.6 kpc which covers the whole narrow line region. Therefore the value of $\mathrm{H}_\beta^{\mathrm{NLR}}$ derived from the decomposition of the line originates in the NLR and is well within the expected limits.

We expect that the line should change in agreement with variations of the nuclear continuum F_{nucl} as follows:

$$\mathrm{H}_\beta(t) = \mathrm{H}_\beta{}^{\mathrm{NLR}} + AF_{\mathrm{nucl}}(t)\,. \tag{1}$$

However, as the observed flux consists of the variable nuclear part and constant contribution of the FC2 component, the observed relation is the following:

$$\mathrm{H}_\beta(t) = A(F_{\mathrm{nucl}}(t) + F_{\mathrm{FC2}}) + B\,. \tag{2}$$

Comparing the two formulae we can estimate the contribution from FC2 component

$$F_{\mathrm{FC2}} = (\mathrm{H}_\beta{}^{\mathrm{NLR}} - B)/A\,. \tag{3}$$

The values of the coefficients A and B are derived directly from the fit of the straight line to the data (Fig. 3). The value of the coefficient B is 1.95×10^{-13} erg/s/cm^{-2} and A is equal to 0.92 in appropriate units.

The value of $\mathrm{H}_\beta{}^{\mathrm{NLR}}$ equal to 1.5×10^{-13} ergs/s/cm^2 gives us the contribution of the FC2 component to the continuum at a level of 0.45×10^{-13} erg/s/cm^2. It is about 20% when the source is weak and drops down to a few percent when it is bright. These values are in agreement with the estimate made by Tran (1995), who showed that the FC2 continuum in Seyfert 1 galaxies account for only about 4% of the total featureless continuum (defined as the sum of nuclear continuum and the scattered, polarized "featureless continuum") while in the Seyfert 2 – for 60%–90%. Therefore, even at its low level, NGC 5548 is not truly approaching Seyfert 2 galaxy properties, although the contribution from FC2 is not completely negligible either.

Unfortunately, we cannot say anything about the shape of the FC2 component since the available off-nucleus spectra are not reliable (see Section 2.2). Therefore, we have to ignore its contribution to the optical/UV spectrum in the next Section.

4. Comparison of the Intrinsic Nuclear Emission with the Accreting Corona Model

We use the determination of the intrinsic nuclear emission to test a specific model of an active nucleus. That model consists of an accretion disk surrounded by a corona, with both an accretion disk and a corona powered directly by accretion

(Życki, Collin-Souffrin and Czerny 1995, Witt, Czerny and Życki 1997). It describes the spectrum of the nuclear emission in the entire optical/UV/X-ray band. The structure of the flow is calculated self-consistently at every radius, as described by Czerny, Witt and Życki (1997), and the emerging spectrum is integrated over the disk surface so the stationary model is characterized by the global parameters: mass of the central black hole, the accretion rate and the viscosity parameter α.

4.1. High and Low State Models

We start with detailed modeling of the two spectra representing a high luminosity state and a low luminosity state. We choose spectra from set A since these are the most reliable (see Section 2.2). IUE data for the high state are also available. In Fig. 5 we show examples of a low (n58733a) and a high (n57649a) flux spectra. The spectra are corrected for starlight, reddening and transformed to rest frame. Unfortunately, they cover only a relatively narrow energy range. In order to show an example of the spectrum covering the entire optical band but to avoid the problem of starlight subtraction in these, not well calibrated, data we plot (see Fig. 6) the difference between the high and low states from set H (n58733h subtracted from n57643h).

The difference between the two states is considerable. For higher states the blue bump becomes more prominent, the H_β line broader, and the underlying continuum changes slope. The data for high and low states are compared with a model of an accretion disk with a hot accreting corona. We adopt the value of the viscosity parameter α equal to 0.1, as suggested by statistical data for quasars (Czerny, Witt and Życki 1997). For such a low viscosity the radial in-fall of mater is accompanied by strong vertical outflow which was included in the model, as described by Witt *et al.* (1997). The best fit to the observed data was obtained for the following parameters: mass of the central black hole $M_{\rm BH} = 1.1 \times 10^8 {\rm M}_\odot$, and the following accretion rates: $\dot{m} = 0.05$ for the high state and $\dot{m} = 0.03367$ for the low state (Fig. 5). The difference between the high and low states resulting from our computations is also plotted against the observed difference (Fig. 6).

In the case of high state the effect of mass loss does not have an important influence on the spectrum. However, in the case of low state the effect is profound so the external accretion rate is only slightly lower than in the high state but the differences in the bolometric luminosities and spectral shapes between the two states are considerable.

The model gives a good fit to the observational data. It also predicts the X-ray flux in the 2–10 keV region. The estimated value of the 2–10 keV flux obtained from the model for the high state is: 2.04×10^{-11} ergs/s/cm^2.

This estimate can be compared with a prediction based on observational data from Clavel *et al.* (1992). The observed (undereddened) UV flux at $\lambda = 1350$ Å ($\log \nu = 15.35$) at that epoch was equal to 5.82×10^{-14} ergs/s/cm^2/Å. For F_λ(1350 Å) of the above value the linear formula gives the X-ray flux equal to 6.64×10^{-11} ergs/s/cm^2.

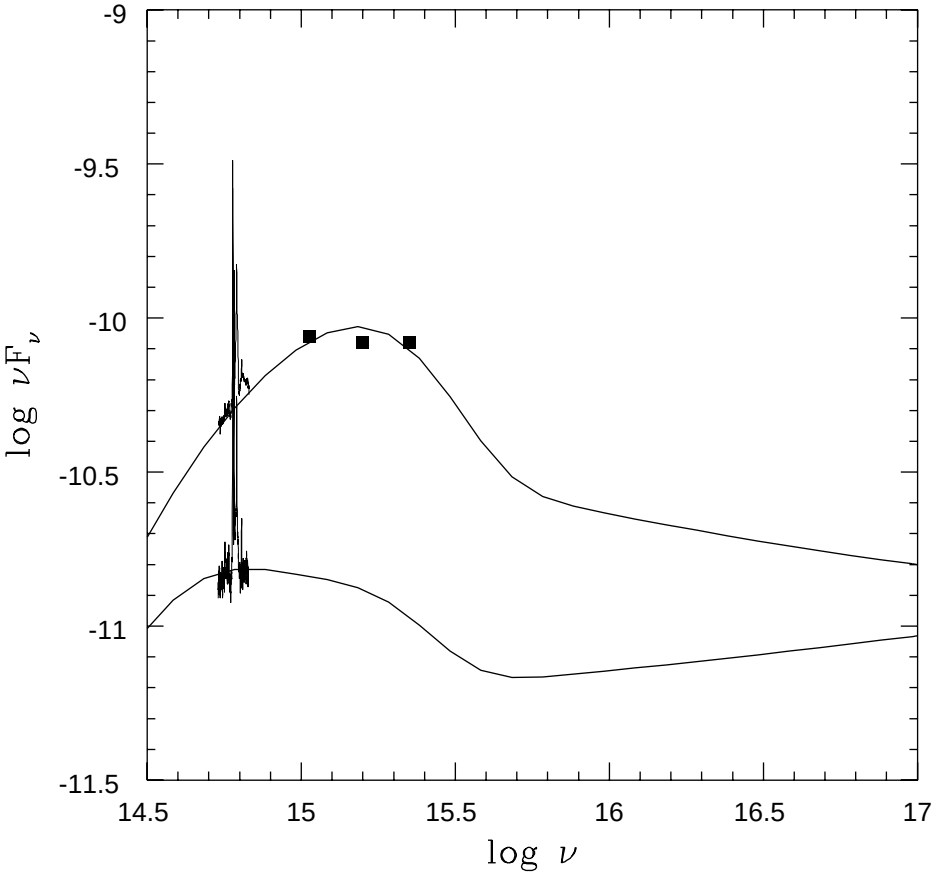

Fig. 5. A low (n58733a) and a high (n57649a) states are shown, starlight subtracted and dereddened and the IUE data points corresponding to the high state. The fitted models are for $M_{\rm BH} = 1.1 \times 10^8 {\rm M}_\odot$, $\alpha = 0.1$ and $\dot{m} = 0.05$, $\dot{m} = 0.03367$ for the high and low state spectra, respectively. Outer disk radius was put at 120 $R_{\rm Schw}$. Fluxes are given in erg/s/cm^2/Hz.

The model therefore is fainter in X-rays than it is expected. Although the linear formula clearly over-predicts the expected value of X-ray flux, as there is a strong flattening in the dependence of the X-ray brightness on the UV flux towards higher UV luminosities, still the required value should be about 5×10^{-11} ergs/s/cm^2, as suggested by visual inspection of Fig. 4 from Clavel *et al.* (1992).

Higher X-ray luminosities for given UV flux are expected from the model if the viscosity parameter is smaller. Adopting $\alpha = 0.05$ we can fit the high state data with the parameters: $M_{\rm BH} = 1.4 \times 10^8 {\rm M}_\odot$, $\dot{M} = 0.037 {\rm M}_\odot$/yr and predict the 2–10 keV flux equal to 3.65×10^{-11} erg/s/cm^2, closer the expectations based on observed trends. However, in that case the required value of the mass of the central black hole becomes somewhat larger than the values between $7 \times 10^7 {\rm M}_\odot$ – $10^8 {\rm M}_\odot$ which resulted from estimates based on the study of the Broad Line Region dynamics (Wanders *et al.* 1995, Done and Krolik 1996; see also Loska and Czerny 1997).

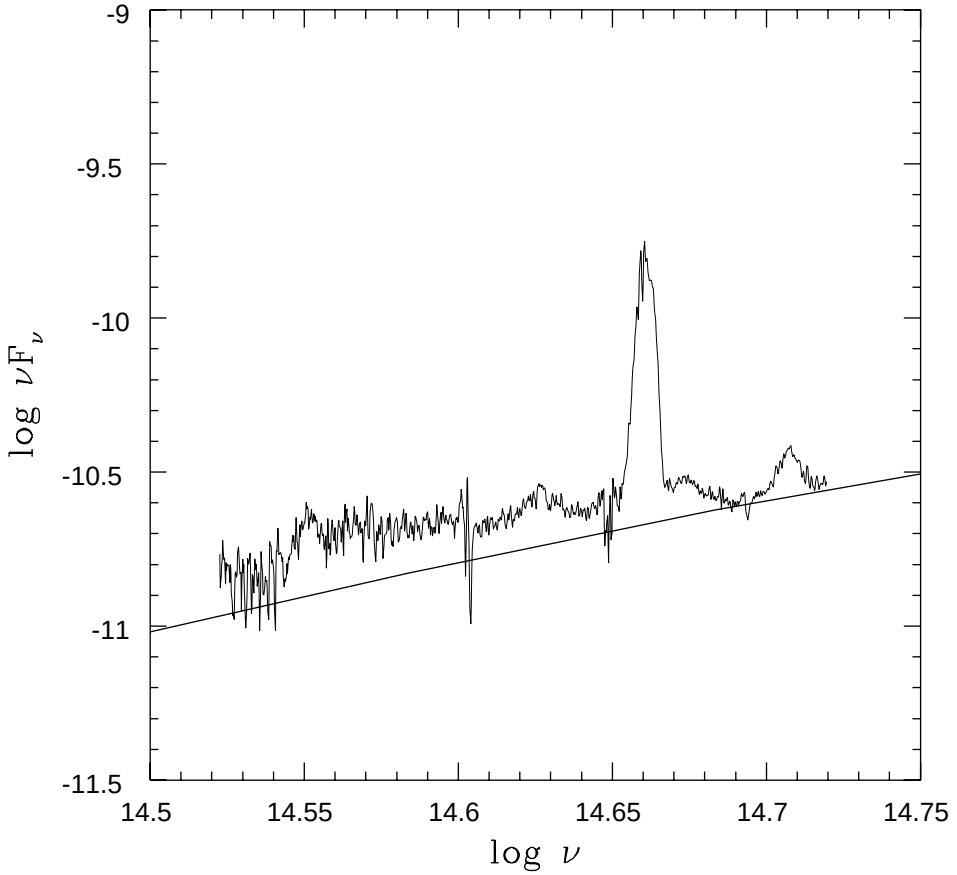

Fig. 6. A broad band difference between two states (n58733h subtracted from n57643h) is shown (in order to avoid stellar subtraction problem), together with the difference between two theoretical spectra from Fig. 5.

4.2. Predicted Dependencies on Accretion Rate

In this Subsection we compare the overall time behavior of the nucleus with predictions of the accreting corona model. We fix the value of the mass of the central black hole M and calculate a sequence of stationary models parameterized by the accretion rate with the spectra covering optical/UV/X-ray band. Therefore, we obtain a theoretical relation between the fluxes at 5100 Å, 1350 Å and the integrated 2–10 keV luminosity, for each M. We compare it with the data from the first year of the observational campaign, when the IUE data were available and with the data of Clavel *et al.* (1992).

The value of the mass $1.1 \times 10^8 \mathrm{M}_\odot$ suggested by the fit to the optical data in a single high state data set does not reproduce well the overall trend (see Fig. 7). Therefore, we also plot a theoretical line corresponding to the central mass of $8 \times 10^7 \mathrm{M}_\odot$ and the viscosity parameter equal to 0.1, as before.

We see that the main trend might be well reproduced assuming a value of the mass of the central black hole about $9.5 \times 10^7 \mathrm{M}_\odot$ which is actually closer to the

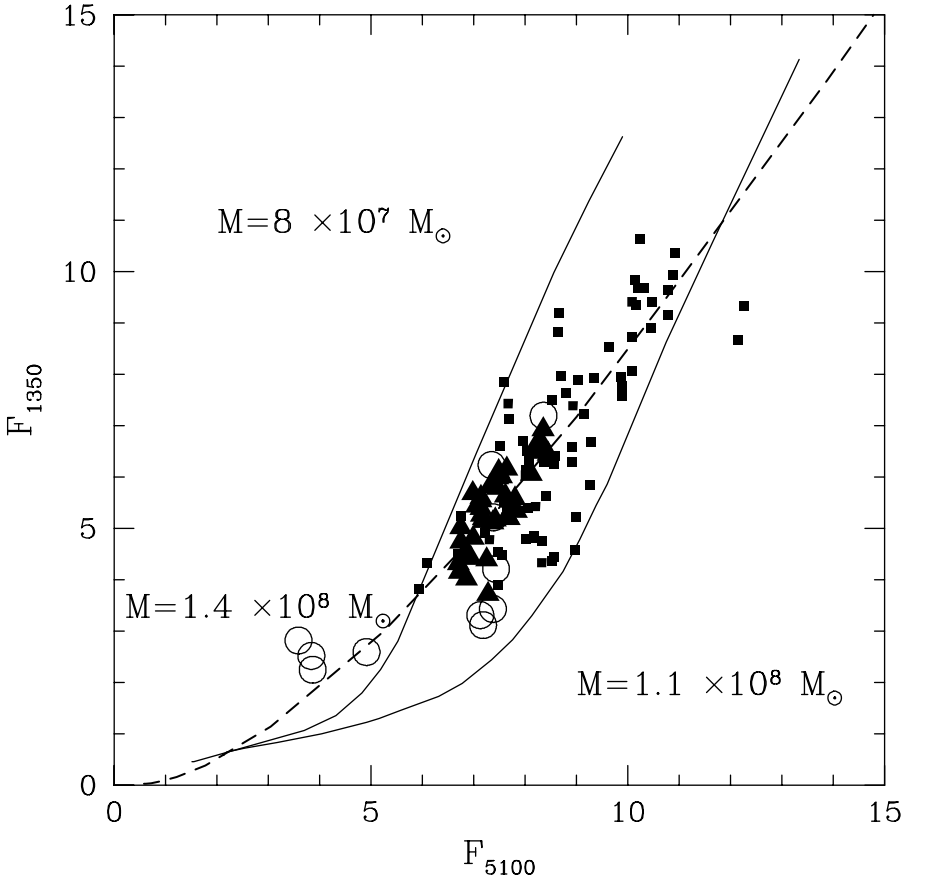

Fig. 7. The relation between the optical and UV flux during the first year of observational campaign given by Clavel *et al.* (1991) (squares) and during the fifth year given by Korista *et al.* (1995) (triangles), after dereddening of the data. Points from July/August 1989 period with exceptionally high H_β are marked by large circles. Continuous lines show the dependence predicted by the model assuming the viscosity parameter equal to 0.1, for two masses of the central black hole. The dotted line marks the predictions for mass loss excluded, black hole mass equal to $1.4 \times 10^8 M_\odot$ and viscosity parameter equal to 0.033. Optical flux is given in units of 10^{-15} erg/s/cm^2/Å, and UV flux in units of 10^{-14} erg/s/cm^2/Å.

value obtained from dynamical considerations. However, smaller mass models lead to even stronger under-production of the X-ray brightness than higher mass models (see Section 4.1).

To inspect the problem of under-production of X-rays we construct a theoretical diagram of the dependence between the UV flux and the integrated flux between 2 and 10 keV (Fig. 8). We add the observational points from Clavel *et al.* (1992). Both families of models from Fig. 7 under-produce the X-ray emission and the predicted character of the dependence is in contrast with the observational points.

Therefore we modified our theoretical model. We neglected the effect of mass loss predicted by the model and used the same value of the accretion rate at all radii for a given external accretion rate. This led to a qualitative change of the shape of the dependence between UV and X-ray flux. We adjusted the mass of the central

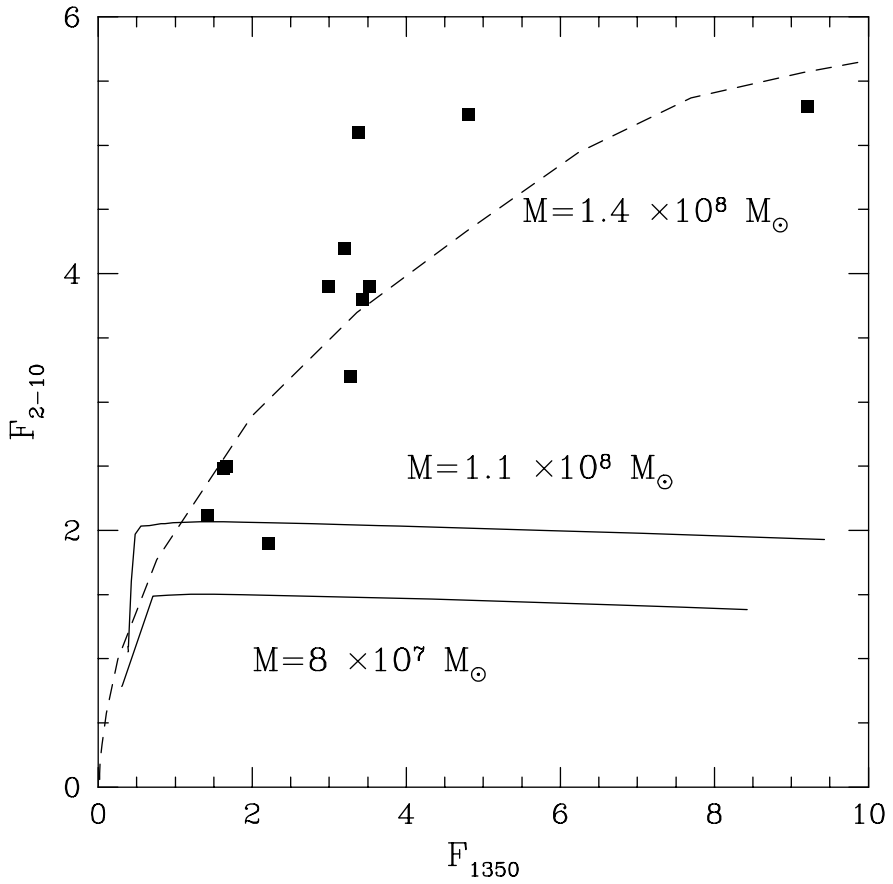

Fig. 8. The relation between the UV flux and the integrated 2–10 keV flux. Data points are from Clavel *et al.* (1992), without dereddening. The brightest point represents the measurement made in 1985. Lines mark the same sets of models as in Fig. 7, but reddened by interstellar extinction. UV flux is given in units of 10^{-14} erg/s/cm^2/Å and X-ray luminosity in units of 10^{-11} erg/s/cm^2/Hz.

black hole to represent well the relation between the optical and UV flux (dashed line in Fig. 7). Additionally, by taking smaller value of the viscosity parameter α we could adjust the level of the X-ray emission to the required level (see dashed line in Fig. 8).

Our modified model of the accreting disk with accreting corona is now consistent with the behavior of all three spectral bands: optical, UV and X-ray, remaining still a two-parameter model, described by the central mass and the viscosity. In the case of NGC 5548 these parameters are: $M_{\rm BH} = 1.4 \times 10^8 {\rm M}_\odot$ and $\alpha = 0.033$.

The spectral range in the optical data without calibration problems (set A) is too short to attempt the distinction between the models with and without mass loss. The model without mass loss, $M_{\rm BH} = 1.4 \times 10^8 {\rm M}_\odot$, $\alpha = 0.033$, and accretion rate $\dot{m} = 0.009$ cannot be visually distinguished from the model given in Fig. 5 (*i.e.*, with mass loss, $M_{\rm BH} = 1.1 \times 10^8 {\rm M}_\odot$, $\alpha = 0.1$. and accretion rate $\dot{m} \approx 0.034$).

We see that the short sequence of points marked with large circles (dates from

7728 to 7766) in Fig. 7 follows approximately the overall trend of the continuum variations although the H_β line response was untypical. Nevertheless, on the basis of Fig. 7 alone we cannot tell what caused the departure of those points from the main trend shown in Fig. 3. Two possibilities are open. Either the line flux was too high (*i.e.*, the BLR did not respond to the decrease of the nuclear emission although the considered period was longer than the usual time delay), or the continuum flux seen by us was too low. This second possibility would happen if some intervening optically thick matter crossed our line of sight.

Although the model of accreting corona is able to reproduce well the broad band time behavior of the nucleus, two problems remain. The first is the question, why the mass loss predicted by the model is possibly too large. The second is that the favored value of the central mass is somewhat larger than suggested by the dynamical studies of the Broad Line Region, although the discrepancy is not stringent.

5. Discussion and Conclusions

5.1. Data Requirements

The character of variability of the Seyfert galaxy NGC 5548 is very complex. It means that the observational data not only have to be distributed densely in time, in order to cover well the short time scale behavior but also have to extend for long times (years) to catch the important long time scale trends. This general problem shows up in a number of particular difficulties.

A few observational points do not always follow the general trend. Two observations made when the emission lines in NGC 5548 were exceptionally weak suggested that the almost complete disappearance of the lines is a break off from the usual behavior of the source (Iijima 1992, Iijima, Rafanelli and Bianchini 1992, Loska, Czerny and Szczerba 1993). Actually, the behavior of the source during that period followed well the general trend, as shown by the continuous frequent sampling (Peterson *et al.* 1994; see also Fig. 3).

On the other hand, there seem to be periods when the source does not follow the typical variability pattern. During the period of about six weeks in July/August 1989 (days 7722 to 7766) the continuum was much fainter than expected on the basis of the H_β intensity. Since the line delay (about 18 days) is much shorter than six weeks the effect cannot be caused by the lack of answer of the Broad Line Region to the change of the continuum. It may suggest some kind of geometrical effect which decreased the level of continuum seen by an observer but not by BLR. However it may also indicate that the coherent response of the BLR require more time than indicated by the measured time delay. In order to avoid problems, we excluded the data collected during that period from our modeling.

In our comparison of the data with the model the observational point in X-rays obtained in 1985 plays a crucial role since the amplitude of the variation reached exceptionally large value at that time. Such events are rare in a sense that large

variations happen in time scales of years but their inclusion in the study is crucial from theoretical point of view so the good data have to cover such long time scales as well as short time scale variability.

The presence of different time scales in the problem is best seen in the study of X-ray power spectra which are basically of a power law shape in all AGN (McHardy and Czerny 1987, Lawrence *et al.* 1987, see also Czerny and Lehto 1997). It is not clear whether the long term variability (in the time scale of years) is actually of the same nature that the best studied variability in time scales of hundreds to thousands of seconds but we cannot *a priori* reject such a possibility and the large amplitude variations like the one mentioned above should be included in any model unless there are arguments against it.

The currently available data on NGC 5548 are already good enough to allow interesting study of the time dependent properties but extension of the observational campaign is essential for better understanding of the behavior of accretion flow.

5.2. Determination of Intrinsic Spectrum of NGC 5548

The results of Section 2 show that the level of starlight at 5100 Å (in the aperture $5\farcs0 \times 7\farcs6$) equal to 3.4×10^{-14} ergs/s/cm^2/Å is determined reliably. However, the spectral shape of the starlight does not seem to be described accurately. Separate spectrophotometric observations of good quality are necessary in order to solve this problem.

The lack of good starlight determination in the entire optical band limits the testing of the model against the data basically to the normalization at 5100 Å. It is not a big problem if the entire optical/UV/X-ray range is studied but nevertheless it makes impossible to use the entire optical range for fine tuning.

The subtraction of the FC2 component is another problem which should be dealt with while fine tuning the model since the level of the FC2 at 5100 Å is up to 20% when the source is exceptionally faint. Fortunately, the source is brighter most of the time so the FC2 contribution could have been neglected in the present analysis of the applicability of the model.

5.3. Model Advantages and Restrictions

The variations of the intrinsic continuum emitted by the nucleus of NGC 5548 in the optical/UV/X-ray band were successfully reproduced using a simple model of an accretion disk with an accreting corona by fixing the mass of the central black hole at $1.4 \times 10^8 M_\odot$ and the viscosity parameter at 0.033 while varying accretion rate from ~ 0.009 to $\sim 0.04 M_\odot$/yr.

The model reproduces well both the hardening of the spectrum with an increase of the luminosity and the weak increase in X-ray luminosity with the increasing UV flux when the source is bright. The disk emission does not extend into soft X-rays so any traces of the soft X-ray excess in this source (Walter and Fink 1993) have to be attributed to the atomic processes connected with reprocessing of X-rays by the disk surface (Czerny and Życki 1994). We neglected those processes in our model

assuming that the disk albedo is equal to zero.

The version of the model which corresponds well to the behavior of the source is the model in which the vertical outflow of the mass from the corona in the form of the wind is neglected. The theory underlying the description of the outflow will have to be reconsidered. Apart from that, the model is a very promising one and should be further tested and developed.

The most important topic is the understanding of the nature of the variations and the character of the global response of the disk/corona system.

In our present approach we simply use a set of stationary models characterized by a single accretion rate at all disk radii at any given moment. This is certainly an oversimplification. The variations in the optical/UV band are noticeable starting from the time scales of one – two days (Korista *et al.* 1995). The main contribution to the spectrum comes from the inner parts of the disk, at radii $r \sim 10\ R_{\rm Schw}$. The thermal time scale of that region depends on the viscosity parameter α and is equal

$$\tau_{th} = 0.2(\frac{0.033}{\alpha})(\frac{M}{1.4 \times 10^8 \mathrm{M}_\odot}) \quad \text{days}$$

and a more accurate value of the two-folding time scale at 1350 Å (independent from the assumption about the disk radius dominating the emission at a given frequency) is equal to $1\overset{\mathrm{d}}{.}0$ for the mean luminosity level (Siemiginowska and Czerny 1989). Therefore, if there are any changes of the corona structure the thermal structure of the disk can follow these changes over the time scales of days.

The viscous time scale is longer than the thermal time scale by a few orders of magnitude (see *e.g.*, Siemiginowska, Czerny and Kostyunin 1996). The disk therefore is never stationary and our assumption is not justified. On the other hand this assumption is the only reasonable approach since we cannot calculate the actual time behavior of the disk because of the lack of proper understanding of the disk/corona coupling. The disk/corona system described by the model is thermally unstable (see Fig. 7 of Witt *et al.* 1997). The sudden increase of the corona activity can therefore result even in enhanced disk response, as required, but this response does not have to saturate at the value of the flux radiated by the disk which is necessary for the corona to reach the new temporary thermal balance. However, if we do assume that the thermal disk runaway saturates at the appropriate emitted flux then the disk/corona structure would be observationally the same as in the case of enhanced accretion rate since the disk/corona coupling does not depend on cold disk structure (surface density etc.).

The applicability of the stationary model to the description of the time evolution suggests that such a saturation actually takes place but its mechanism is unknown. The additional disk/corona coupling might be based on magnetic field and the description of the disk and corona flow by the viscosity coefficient α is too simple to reproduce well the time behavior, including stability, although may approximate the quasi-stationary situation.

Acknowledgements. This research was based on the optical data collected by the AGN Watch team available through private communication with B.M. Peterson. We are grateful to Danusia Dobrzycka, Joanna Mikołajewska and Wojtek Dziembowski for helpful discussions. The project was partially supported by the Polish State Committee for Scientific Research grant 2P03D00410.

REFERENCES

Antonucci, R. 1993, *Ann. Rev. Astron. Astrophys.*, **31**, 473.
Burstein, D., and Heiles, C. 1984, *Astrophys. J. Suppl. Ser.*, **54**, 33.
Clavel, J., *et al.* 1991, *Astrophys. J.*, **366**, 64.
Clavel, J., *et al.* 1992, *Astrophys. J.*, **393**, 113.
Coleman, G.D., Wu, C-C., and Weedman, D.W. 1980, *Astrophys. J. Suppl. Ser.*, **43**, 393.
Czerny, B., Witt, H.J., and Życki, P.T. 1997, in *ESA SP-382*, 2nd INTEGRAL Workshop, "The Transparent Universe", eds. C. Winkler, T. Courvoisier and Ph. Durouchoux, page 397.
Czerny, B., and Lehto, H.J. 1997, *MNRAS*, **285**, 365.
Czerny, B., and Życki, P.T. 1994, *Astrophys. J. Letters*, **431**, L5.
Done, C., and Krolik, J.H. 1996, *Astrophys. J.*, **463**, 144.
Done, C., Pounds, K.A., Nandra, K., and Fabian, A.C. 1995, *MNRAS*, **275**, 417.
Edelson, R., *et al.* 1995, *Astrophys. J.*, **438**, 120.
Iijima, T. 1992, *IAU Circ.*, 5521.
Iijima, T., Rafanelli, P., and Bianchini, A. 1992, *Astron. Astrophys.*, **265**, L25.
Korista, K.T., *et al.* 1995, *Astrophys. J. Suppl. Ser.*, **97**, 285.
Lawrence, A., Pounds, K.A., Watson, M.G., and Elvis, M.S. 1987, *Nature*, **325**, 692.
Loska, Z., Czerny, B., and Szczerba, R. 1993, *MNRAS*, **262**, L31.
Loska, Z., and Czerny, B. 1997, *MNRAS*, **284**, 946.
Marshall, H.L., Fruscione, A., and Carone, T.E. 1995, *Astrophys. J.*, **439**, 90.
McHardy, I.M., and Czerny, B. 1987, *Nature*, **325**, 696.
Osterbrock, D.E. 1989, in "Astrophysics of Gaseous Nebulae and Active Galactic Nuclei" p. 346.
Peterson, B.M., *et al.* 1991, *Astrophys. J.*, **368**, 119.
Peterson, B.M., *et al.* 1992, *Astrophys. J.*, **392**, 470.
Peterson, B.M., *et al.* 1994, *Astrophys. J.*, **425**, 622.
Reichert, G.A., *et al.* 1994, *Astrophys. J.*, **425**, 582.
Reynolds, C.S. 1997, *MNRAS*, **286**, 513.
Romanishin, W., *et al.* 1995, *Astrophys. J.*, **455**, 516.
Seaton, M.J. 1979, *MNRAS*, **187**, 73P.
Serote-Ross, M., Boisson, C., Joly, M., and Ward, M.J. 1996, *MNRAS*, **278**, 897.
Siemiginowska, A., and Czerny, B. 1989, *MNRAS*, **239**, 289.
Siemiginowska, A., Czerny, B., and Kostyunin, V. 1996, *Astrophys. J.*, **458**, 491.
Stripe, G.M., *et al.* 1994, *Astrophys. J.*, **425**, 609.
Tran, H.D. 1995, *Astrophys. J.*, **440**, 597.
Walter, R., and Fink, H.H. 1993, *Astron. Astrophys.*, **274**, 105.
Wamsteker, W., *et al.* 1990, *Astrophys. J.*, **354**, 446.
Wanders, I., *et al.* 1995, *Astrophys. J.*, **453**, L87.
Wills, B.J., Netzer H., and Wills, D. 1985, *Astrophys. J.*, **288**, 94.
Witt, H.J., Czerny, B., and Życki, P.T. 1997, *MNRAS*, **286**, 848.
Yee, H.K., and Oke, J.B. 1978, *Astrophys. J.*, **226**, 763.
Zheng, W., *et al.* 1995, *Astrophys. J.*, **44**, 632.
Życki, P.T., Collin-Souffrin, S., and Czerny, B. 1995, *MNRAS*, **277**, 70.